INTERNATIONAL JOURNAL OF AUTOMOTIVE AND MECHANICAL ENGINEERING (IJAME)
ISSN: 2229-8649 e-ISSN: 2180-1606
VOL. 18, ISSUE 3, 9042 – 9050
DOI: https://doi.org/10.15282/ijame.18.3.2021.16.0693

ORIGINAL ARTICLE

Finite Element Analysis to Determine Stiffness, Strength, and Energy Dissipation of U-Shaped Steel Damper under Quasi-Static Loading

E. Satria*, L. Son, M. Bur and M. Dzul Akbar

Structural Dynamics Laboratory, Department of Mechanical Engineering, Universitas Andalas, Kampus Limau Manis Padang, Sumatera Barat, Indonesia, 25163
Phone: +6275172947; Fax: +6275172566

ABSTRACT – In seismic areas, the application of structural dampers becomes compulsory in the design of buildings. There are various types of dampers, such as viscous elastic dampers, viscous fluid dampers, friction dampers, tune mass dampers, yielding/ metallic dampers, and magnetic dampers. All damper systems are designed to protect structural integrities, control damages, prevent injuries by absorbing earthquake energy, and reduce deformation. This paper is a part of research investigating the behaviour of the U-shaped steel damper (as one type of metallic damper) that can be applied to the buildings in seismic areas. The dampers are used as connections between the roof and supporting structure, with the two general purposes. The first is to control the displacement of roof under an earthquake, and the second is to absorb seismic energy through the plasticity of some parts in dampers. If a strong earthquake occurs, the plasticity will absorb the seismic energy; therefore, heavy damage could be avoided from the roof's mainframes. In this paper, several models of U-shaped steel dampers are introduced. Several parameters, such as elastic stiffness, maximum strength, and energy dissipation, are determined under two conditions. Firstly, static analysis of the proposed damper under variation of U-steel plate configurations, searching the model with more significant energy dissipation. Secondly, static analysis of the unsymmetrical and symmetrical damper under different loading directions. An in-house finite element program that involves both geometrical and material nonlinearities is developed as a problem solver. A quasi-static lateral loading is given to each model until one cycle of the hysteresis curve is reached (in the displacement range between -20 mm to +20 mm). The above parameters are calculated from the hysteresis curve. From the results, the behaviour of the U-steel damper can be described as follows. Firstly, increasing the energy dissipation in the lateral direction can be done by increasing the lateral stiffness of the damper. However, it can reduce the maximum elastic deformation of the damper. Secondly, under the random direction of loading, a symmetrical shape can increase the energy dissipation of the damper.

ARTICLE HISTORY
Received: 5th Feb 2021
Revised: 10th Aug 2021
Accepted: 11th Sept 2021

KEYWORDS
U-shaped steel damper;
Stiffness;
Strength;
Energy dissipation;
Finite element analysis

INTRODUCTION

This paper is a part of a series of studies to improve the design of space structures, particularly in seismic areas. In terms of geometry and dimension optimisation, the first study was conducted to find the optimum geometry of the structures with the highest strength under loading. This study applied a form-finding method to resist the given external loads such as self-weight, wind, earthquake, and snow [1]. Then, another numerical study, called member proportioning, was aimed to reduce the thickness of the uncritical members of the space structures; therefore, the systems can be made lighter [2]. In terms of damage controller, several previous studies focused on searching for a mechanism that can be acted as a damper and as an energy absorber at the same time. The first studies introduced a T-joint strut in the structures of a two-way single-layer lattice dome with eccentricity [1], [2]. The studies showed the feasibility of T-joint struts to reduce the displacement and absorb earthquakes' energy through the yielding of T-joints.

Some previous research introduced energy absorber models in buildings, especially in Passive Energy Dissipating Devices (PED). PEDs are mechanical devices to dissipate or absorb a portion of structural input energy, thus reducing structural response and possible structural damage. Several types of PED, such as base isolation, friction dampers, metallic dampers, viscous elastic dampers, viscous fluid dampers, tuned mass dampers, and tuned liquid dampers, are introduced. A new approach to base isolation for reducing the earthquake's destructive effect has been proposed using a pendulum isolator. In this method, the basements that have spherical surfaces are used as base isolation. A study done by Spuler et al. [3] introduced several pendulum isolators: a single primary sliding surface, dual primary sliding surfaces, and a combination of single and double sliding surfaces. Applications of these isolators in the building, such as in Greek National Opera (Greece), Timsah Arena (Turkey), and Fairmont Hotel (UAE), have also been generally discussed in the study. Another type of PED is a friction damper. The friction damper operates on a coulomb damper or friction brake principles, translating kinetic energy into heat by friction. Armali et al. discussed the effectiveness of using friction dampers as PED and proposed some design optimisation of the number and position of dampers in the building [4].

*CORRESPONDING AUTHOR | E. Satria | ekasatria@eng.unand.ac.id

Other PED types are viscous elastic damper and viscous fluid damper. A viscous elastic damper converts a portion of mechanical energy into heat energy through viscoelastic material, as a medium in which energy transfer occurs. A study done by Shedbale et al. [5] reviewed several types of viscous elastic dampers and the used materials to dissipate energy. Another study by Ras and Boumechra [6] investigated seismic energy dissipation for viscous fluid dampers in the steel structure design. Fluid viscous dampers work based on the principle of dissipation of energy because of fluid flowing through orifices. This study analysed the steel structure behaviour with and without viscous fluid dampers for a 12-story building using engineering software. The result showed that viscous fluid dampers in buildings reduced the structural response compared to the unbraced ones.

Other PED types are tuned mass damper (TMD) and tuned liquid damper (TLD). TMD consists of a vibrating mass that moves out of phase with the motion of the structure attached. As it moves out of phase, the TMD system's inertial force dissipates the energy and reduces the structure's vibrations. TMD was more effective when attached to the top floor of the building [7]. Its application can prevent discomfort, damage, or outright structural failure. A study was done by Rahimi et al. [8] reviewed many types of TMD in protecting structures from unpredictable vibrations. Their paper presented critical reviews and comparative studies of active, passive, semi-active, and hybrid control systems of TMD. Since early 1970, TMDs have been considered as the ingenious system for passive vibration control of many buildings [9]. They have been installed in many high-rise buildings, such as John Hancock Tower in Boston and Citicorp Center in New York City [10], Sidney Tower in Australia, Chiba Port Tower, and Fund Bridge in Japan [11] and Taipei Tower in Taiwan [12]. To improve the application of TMD, especially under earthquake with many modes, a multiple tuned mass damper (MTMD) has been introduced [13], [14].

On the other side, TLD is less commonly used than TMD to reduce the vibration of slender structures. A TLD is a container that is partially filled with a mixture of water and glycol. It has no moving parts; the sloshing of the internal liquid provides the damping. The most popular type of TLD is tuned liquid column damper (TLCD). TLCD is a U-shaped tube filled with fluid. Liquid flows from one vertical column to the other, creating horizontal damping force due to impact on vertical walls and friction between liquid and tube in horizontal part [15]. Many studies have been developed in TLCD, such as Farshidianfar et al. [16] investigated the optimal parameter's design of TLCD, such as tuning frequency ratio, length ratio, and mass ratio. These parameters were obtained by using the white noise type of wind excitation. Son et al. [17] produced one type of TLCD using a water vibration system in a U-shaped container for a two-story building model. Park et al. [18] proposed a damping mechanism using embossments on the wall of the TLCD, known as ETLCD, to control the vibration of the tall buildings. They found that the performance of ETLCD is superior compared to the conventional TLCD. Moreover, in terms of the combination of TMD and TLD, a study done by Son et al. [19] investigated the behavior of dynamic vibration absorbers that consisted of TMD and TLD to reduce the vibration response in a two-story building model. Another study done by Di Matteo et al. [20] examined control performances of the combined devices analytically and experimentally.

The most developing type of PED is a metallic damper. This damper relies on the principle that the metallic device deforms plastically to dissipate the earthquake's energy. Aghlara et al. [21] conducted a comparative study of eight metallic yielding dampers based on four parameters: equivalent viscose damping ratio, large load to weight, ductility, and cumulative displacement. The reviewed dampers are as follows: a steel triangular-plate added damping and stiffness (TADAS) device, the cast steel yielding brace system (YBS), two passive earthquake energy dissipative devices (dual-pipe damper (DPD) and infilled-pipe damper (IPD)), the yielding shear panel device (YSPD), hysteretic steel damper (HSD), dual-function metallic dampers (Single Round Hole (DFMD-O) and Double X-Shaped (DFMD-X)). The comparative study has shown a correlation between the equivalent damping ratio, energy dissipation capacity, and the energy dissipation mechanism used in a damper. The newest study, done by Javanmardi et al. [22], presented a comprehensive state-of-the-art review of the development and application of metallic dampers. The review discussed the metallic dampers in many aspects, such as materials, analysis through computational methods, manufacturing, and implementation.

This paper examines the metallic damper's mechanical characteristics in a U-shaped steel damper under quasi-static analysis through numerical calculation. The proposed damper is placed between roof structures and building base structures. An initial study was conducted to investigate the mechanical characteristic of the damper to reduce the displacement [23]. Through this study, the stiffness and energy dissipation of the damper under cyclic loading were calculated numerically. These parameters are then used in dynamic analysis of two degrees of freedom of the spring-mass system, representing a roof and building model. The result showed that the displacement of the roof model could be reduced with the application of the proposed damper. The current study focuses on investigating the mechanical characteristics of the damper under variation of stiffness and loading directions. Variation of the stiffness is given by adding U-steel plates to the basic model; therefore, three damper configurations are introduced. Variation of loading direction is shown due to the random direction of the earthquake. This study uses a numerical approach based on nonlinear finite element analysis to determine the mechanical properties of the damper, such as elastic stiffness, maximum strength, maximum elastic displacement, and energy dissipation.

RESEARCH METHODOLOGY

Stage 1: Development of Numerical Models of U-Shaped Steel under Variation of Configuration

The U-shaped steel damper was modelled as presented in Figure 1. Generally, the structure has three main parts: upper and lower steel plates and U-steel plates. Both upper and lower steel plates have a function to hold a set of U-steel plates through-bolt connections. The connections are assumed very rigid. The U-steel plate is the central part of the damper to reduce the displacement and absorb energy through its yielding. In the numerical model, both the upper and lower plates are assumed very rigid; therefore, no yielding occurs in the plates. Stage 1 aims to determine the elastic stiffness, maximum strength, maximum elastic displacement, and energy dissipation of the damper under variation of the configuration of U-shaped steels.

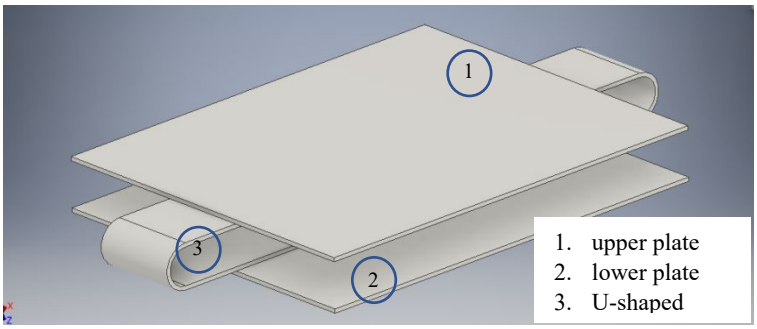

Figure 1. U-shaped steel damper.

Geometrical properties of U-shaped steel dampers

In this part, the U-steel damper configurations are divided into three models, as presented in Figure 2. Then, the U-steel plate dimensions are generally described based on Figure 3, and the details are given in Table 1. The essential consideration of selecting these three models is finding the configuration with more significant energy dissipation. There are three configurations introduced. Model_11 is a basic model with a pair of U-plate given on the damper's left and right sides. Model_12 can considerably increase the stiffness and maximum strength of the damper in the horizontal direction; therefore, the area of the hysteresis curve will be larger (meaning more significant energy dissipation). Model_13 is also considerably able to increase the stiffness of the damper (especially in the vertical direction) and increase the maximum elastic deformation. Therefore, hypothetically, it is also possible to get a more significant energy dissipation.

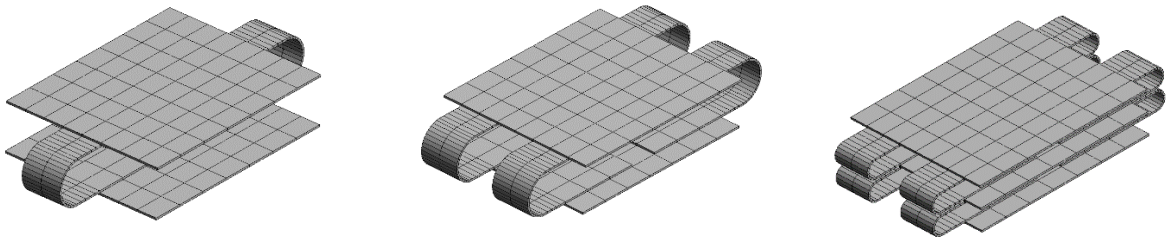

(a) (b) (c)

Figure 2. Variation of configurations of U-shaped steel damper. (a) Model_11: A pair of U-steel plate configurations, (b) Model_12: Two-pairs of U-steel plate configuration, (c) Model_13: Double two-pairs of U-steel plate configuration.

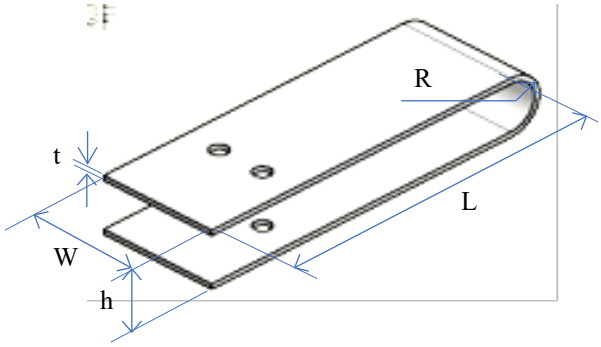

Figure 3. U-shaped steel dan its parameter.

Table 1. Dimension for U-steel plate of Stage 1.

Parameters	Values (mm)
Length, L	125
Radius, R	75
Width, W	90
Height, h	150
Thickness, t	10

Modelling of load and boundary condition

Material properties of the U-shaped steel plate and holding plates are given in Table 2. Modelling of load and boundary conditions (BC) are presented in Figure 4. Loading is initially given in a positive X-axis direction until displacement reaches 20 mm. The direction of loading is reversed to a negative X-axis direction until -20 mm (until reaching one cycle of hysteresis). The load P is only given in X-direction (θ=0°). The 20 mm of maximum displacement is selected to make sure plasticisation has occurred. The upper plate is permitted to displace horizontally; therefore, all nodes in that plate are allowed to displace in X- and Z-direction. The lower plate is restrained from displacement in all directions (fixed); therefore, all nodes in that plate are restrained from displacing in X-, Y- and Z-directions.

Table 2. Material properties.

Parameters	Values
Modulus of elasticity, E	210000 MPa
Shear modulus, G	7900 MPa
Yield strength, σ_y	270.1 MPa
Poisson's ratio, v	0.3
Stress-strain relationship	Bi-linear

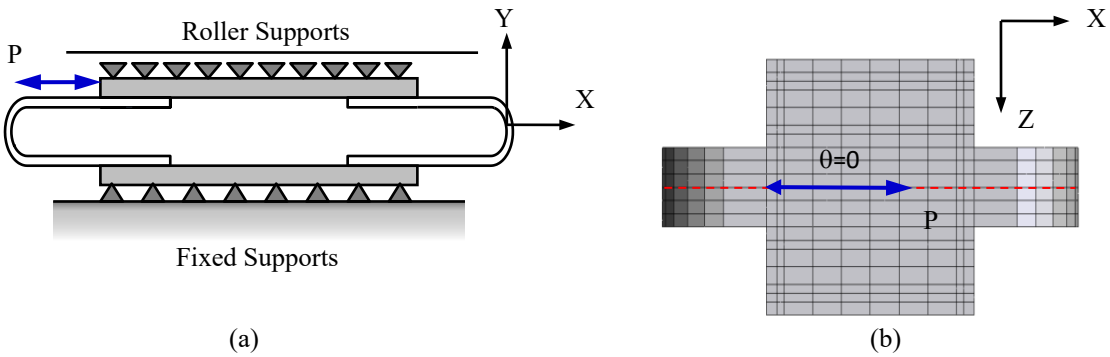

Figure 4. (a). Modelling of load and boundary conditions, and (b) variation of loading direction.

Stage 2: Development of Numerical Models of U-Shaped Steel Damper under Variation of Loading Direction

Stage 2 aims to determine the elastic stiffness, maximum strength, maximum elastic displacement, and energy dissipation of the damper under variation of loading direction.

Geometrical properties of U-shaped steel dampers

In this part, the U-steel damper configuration is given in two models, as presented in Figure 5. Then, the dimensions of the U-steel plate are given in Table 3. The essential consideration of selecting these two models is described as follows. Model_21 is chosen as the unsymmetrical model of the damper, where Model_22 is chosen as the symmetrical model of the damper. Due to the direction the earthquake could be acted randomly, this section aims to investigate the effect of loading direction on mechanical characteristics of the models, especially their energy dissipation.

Table 3. Dimension for U-steel plate of Stage 2.

Parameters	Values (mm)
Length, L	362
Radius, R	33.5
Width, W	125
Height, h	67
Thickness, t	6

(a) (b)

Figure 5. Variation of configurations of U-shaped steel damper (a) Model_21: A pair of U-steel plate configurations on one side of the damper, representing unsymmetrical damper, (b) Model_22:Two-pairs of U-steel plate configurations on both sides of the dampers, representing symmetrical damper.

Modelling of load and boundary condition

These material properties are similar to Stage 1, as can be seen in Table 2. Modelling boundary conditions are similar to Stage 1, as described in Figure 4(a). The only difference is the modelling of load given in two directions: X- and Z-direction. The direction of loads is presented in a variation of θ=0°, 30°, 45°, 60° and 90°, from both X- and Z-axes, as seen in Figure 6.

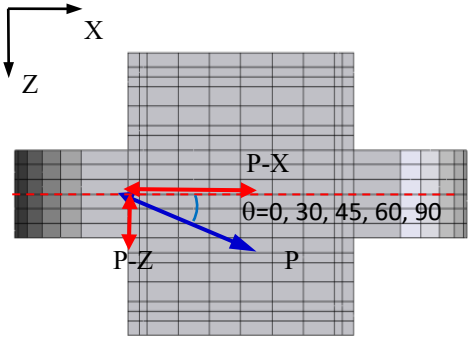

Figure 6. Modelling of load.

Stage 3: Development of Computational Program based on Finite Element Analysis

A computer program based on the nonlinear finite element concept had been developed to analyse the stiffness and strength of a U-shaped steel damper. This damper is modelled by 20 nodes-hexahedron elements. This program was built by involving nonlinearities of geometry and material. A geometrical nonlinearity is calculated based on Updated Langrangian Jaumann by considering large rotation and displacement, whereas a material nonlinearity is calculated using the yield criterion of Von Misses, associated flow rule, and hardening rule. A numerical solution is solved by applying a displacement control method.

Several considerations are made in the finite element modelling of a U-shaped steel damper. First, a contact problem between sliding plates (upper and lower plate) and deformable plate (U-shaped steel) is not considered. Second, friction forces between the sliding plate and deformable plate are neglected, and third, the residual stresses are also neglected in the numerical simulation. The computational program has been used to analyse many structures under various study cases [23]-[25]. The results have been verified very well by theoretical calculation as well as experiments.

Governing finite element equation considering large deformation

The incremental equilibrium equation of the solid structure is written in the equation below.

$$([\mathbf{K_L}] + [\mathbf{K_{NL}}])\{\Delta \boldsymbol{u}^{\boldsymbol{k}}\} = \{\Delta P\} \tag{1}$$

The stiffness matrix of the structure consists of two major parts: $[\mathbf{K_L}]$ is a linear stiffness matrix as in the case of small deformation, and $[\mathbf{K_{NL}}]$ is a nonlinear stiffness matrix due to large deformation and $\{\Delta P\}$ is the residual force from time 't' to 't+Δt'.

$$[\mathbf{K_L}] = \int_V [\mathbf{B_L}]^{\mathbf{T}}[\mathbf{E}][\mathbf{B_L}]\boldsymbol{dV} \tag{2}$$

$$[\mathbf{K_{NL}}] = \int_V [\mathbf{B_1}]^{\mathbf{T}}[\boldsymbol{\sigma}][\mathbf{B_1}]\boldsymbol{dV} - \int_V \mathbf{2}[\mathbf{B_2}]^{\mathbf{T}}[\boldsymbol{\sigma}][\mathbf{B_2}]\boldsymbol{dV} \tag{3}$$

$$\{\Delta P\} = \mathrm{R}(\mathrm{t}+\Delta\mathrm{t}) - \int_{V} [\mathbf{B_L}]^{\mathbf{T}}\{\boldsymbol{\sigma}\}\boldsymbol{dV} \tag{4}$$

$[\mathbf{B_L}]$ is a linear strain displacement transformation matrix, $[\mathbf{B_1}]$ and $[\mathbf{B_2}]$ are geometric matrices due to large deformation. $[\boldsymbol{\sigma}]$ and $\{\boldsymbol{\sigma}\}$ are Cauchy stress matrix and vector at time 't' respectively.

Elastoplastic constitutive relations

For steel material, the Von Misses yield criterion with mixed hardening model can be written in the general form.

$$\mathrm{F}\left(\sigma,\alpha,\varepsilon_{\mathrm{p}}\right) = \mathrm{f}(\sigma,\alpha) - \mathrm{Y}\left(\bar{\varepsilon}_{\mathrm{p}}\right) = 0 \tag{5}$$

Parameter $\mathrm{f}(\sigma,\alpha)$ is a stress function equal to the effective stress or equivalent stress and defines the shape of the yield surface, $\mathrm{Y}\left(\bar{\varepsilon}_{\mathrm{p}}\right)$ represents the size of the yield surface and is a function of $\bar{\varepsilon}_{\mathrm{p}}$ (called the effective strain), and α is the hardening parameter.

$$\mathrm{f}(\sigma,\alpha) = \begin{bmatrix} \frac{1}{2}\left[(\sigma_x-\sigma_y)-(\alpha_x-\alpha_y)\right]^2 + \left[(\sigma_y-\sigma_z)-(\alpha_y-\alpha_z)\right]^2 \\ +\left[(\sigma_z-\sigma_x)-(\alpha_z-\alpha_x)\right]^2 + \\ 6\left[(\tau_{xy}-\alpha_{xy})^2+(\tau_{yz}-\alpha_{yz})^2+(\tau_{zx}-\alpha_{zx})^2\right] \end{bmatrix}^{\frac{1}{2}} \tag{6}$$

$$\mathrm{Y}\left(\varepsilon_{\mathrm{p}}\right) = \mathrm{Y}_1 + \mathrm{H_i}\left(\bar{\varepsilon}_{\mathrm{p}}\right) \tag{7}$$

Parameter Y_1 is the initial yield stress, and $\mathrm{H_i}$ is an isotropic strain hardening function of $\bar{\varepsilon}_{\mathrm{p}}$. The incremental stress-strain relation can be calculated as follow

$$\{\mathrm{d}\sigma\} = \left[D_{ep}\right]\{\mathrm{d}\varepsilon\} \tag{8}$$

$$\left[\mathrm{D_{ep}}\right] = [\mathrm{D_e}] - \frac{[\mathrm{D_e}]\{\partial \mathrm{f}/\partial\sigma\}\{\partial \mathrm{f}/\partial\sigma\}^T[\mathrm{D_e}]}{\mathrm{H}' - \{\partial \mathrm{f}/\partial\sigma\}^T[\mathrm{D_e}]\{\partial \mathrm{f}/\partial\sigma\}} \tag{9}$$

$[\mathrm{D_e}]$ and $\left[\mathrm{D_{ep}}\right]$ are linear and elastoplastic constitutive matrices, H' is a total plastic modulus, and $\{\partial \mathrm{f}/\partial\sigma\}$ is a flow vector. The flow vector is expressed as Eq. (10) below.

$$\{\partial \mathrm{f}/\partial\sigma\}^T = \frac{3}{2\bar{\sigma}}\{\sigma_x'-\alpha_x' \quad \sigma_y'-\alpha_y' \quad \sigma_z'-\alpha_z' \quad 2(\tau_{xy}'-\alpha_{xy}') \quad 2(\tau_{yz}'-\alpha_{yz}') \quad 2(\tau_{xz}'-\alpha_{xz}')\} \tag{10}$$

$\bar{\sigma}$ is an effective strain.

RESULTS AND DISCUSSION

Characteristics of U-Damper under Variation of Configurations

Table 4 shows the elastic stiffness, maximum strength, maximum elastic deformation, and energy dissipation values of the analysed hysteretic steel damper for three models under various configuration variations. Model_11, considered the basic model, gives 4593 N/mm of elastic stiffness and 19741 N of maximum strength. There are two variations of configuration that have been proposed. First, by increasing the numbers of U-shaped steel horizontally, as shown in Model_12, the elastic stiffness increases to be 9891 N/mm, and maximum strength also increases to be 37980 N/mm. Second, by increasing numbers of U-shaped steel vertically, as shown in Model_13. The result shows that the elastic stiffness decreases to be 4662 N/mm, the maximum strength slightly decreases to be 35455 N, but the maximum elastic deformation increases significantly to be 8 mm. From the comparison, as seen in Figure 7, it can be seen that Model_12 can improve the damper's characteristic in terms of horizontal elastic stiffness. In contrast, Model_13 can improve the damper's characteristic in terms of maximum elastic deformation.

Table 4. Elastic stiffness, maximum strength, and energy dissipation of U-shape steel dampers under variation of damper's configuration.

Model	Elastic stiffness, K_{LIN} (N/mm)	Max. strength, P_Y (N)	Max. displacement, δ (mm)	Energy dissipation, E (N.mm)
Model_11	4953.84	19741.73	4.65	1356423.30
Model_12	9891.07	37980.42	4.40	2711176.17
Model_13	4662.07	35455.93	8.00	1660198.06

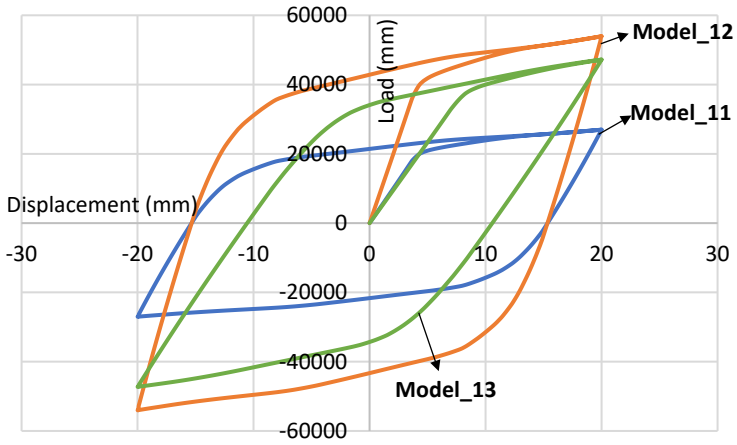

Figure 7. Comparison of curves of load-displacement under variation of the configuration.

Table 4 and Figure 7 also show the value of energy dissipation from all models. Energy dissipation is a sum of energy from the external load that the damper can absorb through yielding. Each model's energy dissipation value will determine the damper's ability to absorb energy. These values are numerically calculated from the area of hysteresis curves for each model. A larger area means the damper's ability to absorb the earthquake's energy will be better; therefore, any damages could be minimised. Model_12 shows the largest area of the hysteresis curve, which means it has the highest energy dissipation (2711176.17 N.mm) compared to Model_11 (1356423.30 N.mm) or Model_13 (1660198.06 N.mm).

Characteristics of U-Damper under Variation of Loading Direction

In this section, the damper's characteristics are determined based on the variation of the cyclic loading direction. The angle is varied in 5 values, θ=0°, 30°, 45°, 60° dan 90°. The hysteresis curves for all models are provided in Figure 8 and Figure 9. Table 5 shows the elastic stiffness K_{LIN} in X and Z-direction for the two models. In general, it can be said that for both models, the increasing angle of θ reduces the elastic stiffness in X-direction, but on the contrary, increases the elastic stiffness in Z-direction. The difference between them is that, for unsymmetrical damper (Model_21), the elastic stiffness in Z-direction is bigger than stiffness in X-direction (5578.09 N/mm compared to 1991.47 N/mm). On the other side, for the symmetrical damper (Model_22), the elastic stiffness in Z-direction is almost similar to the elastic stiffness in X-direction (7592.14 N/mm compared to 8770.52 N/mm). Although there are still minor differences, in general, the tendency of results has shown symmetrical behaviour.

Then, Table 5 also shows the values of maximum strength, P_Y, for both models. In general, this parameter's tendency is similar to elastic stiffness, where the increasing angle of θ reduces P_Y in the X-direction and, on the contrary, will increase P_Y in the Z-direction. The value of P_Y in X-direction will be maximum at θ = 0° (13701.7 N for Model_21 and 28942.7 N for Model_22). On the other hand, P_Y values in the Z-direction is maximum at θ = 90° (18407.7 N for Model_21 and 28850.1 N for Model_22). Again, for symmetrical damper (Model_22), the tendency of these values is almost similar.

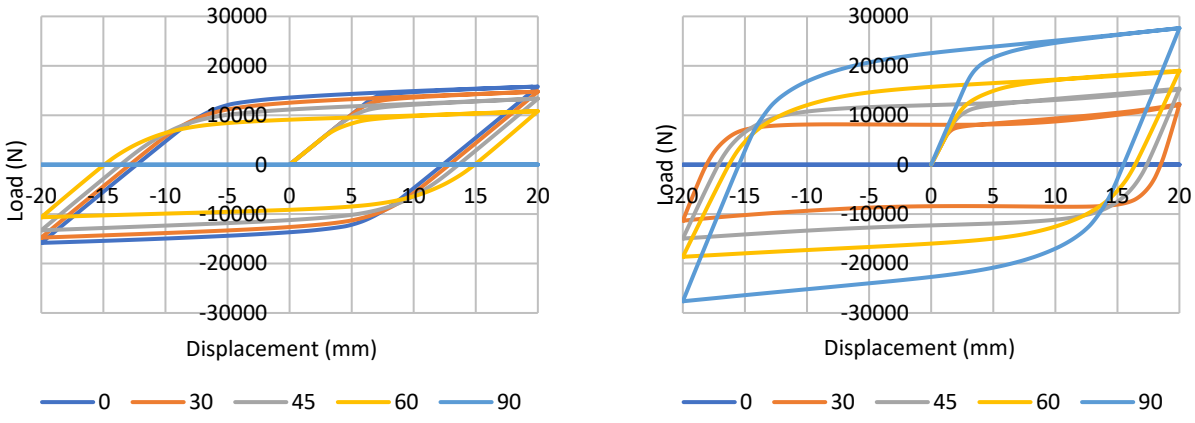

Figure 8. Hysteresis curve for Model_21 (unsymmetrical damper) under variation of loading directions (a) in X-direction, and (b) Z-direction.

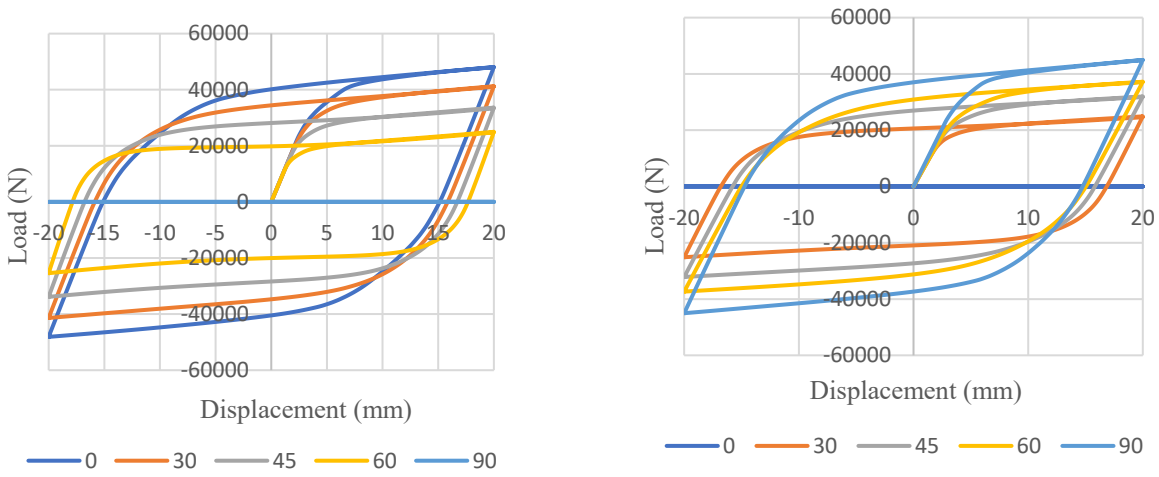

Figure 9. Hysteresis curve for Model_22 (symmetrical damper) under variation of loading directions (a) in X-direction, and (b) Z-direction.

Table 5 shows the energy dissipation (E) values in X- and Z-directions for both models. In general, this parameter's tendency is similar to elastic stiffness, where the increasing angle of θ reduces E in the X-direction and, on the contrary, increases E in the Z-direction. For Model_21, the energy dissipation is different for each loading direction. For example, the value of E-Z for θ = 90° is 1395.08×10^3 N.mm. It is more significant than E-X for θ = 0° (669.28 ×10^3 N.mm). However, for Model_22, the energy dissipation is almost similar for θ = 0°, 45°, and 90° due to the symmetrical geometry of the U-shaped damper. For example, the energy dissipation of E-Z for θ = 90° is 2157.36×10^3 N.mm, which is almost similar to E-X for θ=0° (2340.51 N).

Table 5. Elastic stiffness, maximum strength, and energy dissipation of U-shape steel dampers under variation of loading directions.

Model	θ (°)	K_{LIN}–X (N.mm)	K_{LIN}–Z (N.mm)	P_Y–X (N)	P_Y–Z (N)	E–X (×10^3 N.mm)	E–Z (×10^3 N.mm)
Model_21	0	1991.47	0.00	13701.7	0.00	669.28	0.00
	30	1965.14	4095.74	12563.5	7167.5	657.38	656.09
	45	1902.41	4366.95	10177.9	9607.3	606.90	840.77
	60	1842.60	4547.21	6799.1	11140.7	533.35	1009.52
	90	0.00	5578.09	0.00	18407.7	0.00	1395.08
Model_22	0	8770.52	0.00	28942.7	0.00	2340.51	0.00
	30	8714.20	6652.25	25706.9	15300.2	2118.78	1345.57
	45	8166.08	6510.43	22048.4	20833.4	1809.99	1643.17
	60	8421.23	6129.40	14737.2	25436.9	1373.52	1800.42
	90	0.00	7592.14	0.00	28850.1	0.00	2157.36

CONCLUSION

In this paper, several models of U-shaped steel dampers are introduced. Several parameters, such as elastic stiffness, maximum strength, and energy dissipation, are determined under two conditions. Firstly, static analysis of the proposed damper under variation of U-steel plate configurations, searching the model with more significant energy dissipation. Secondly, static analysis of the unsymmetrical and symmetrical damper under different loading directions, finding the effect of geometrical shape on the dissipation energy. The results are presented as follows:

i. Increasing the number of U-shaped steel in the horizontal direction can improve the horizontal elastic stiffness and maximum strength; therefore, the area inside the hysteresis curve can be made larger, meaning more significant energy dissipation. However, the maximum elastic deformation of the damper will be smaller due to high elastic stiffness. On the other hand, an increasing number of U-shaped steel vertically can increase the maximum elastic deformation in the horizontal direction. However, the elastic stiffness and maximum strength in the horizontal direction decreased. As a consequence, the energy dissipation is less significant than the first model.
ii. Under the random direction of loading, a symmetrical damper gives more significant energy dissipation than an unsymmetrical one.

ACKNOWLEDGEMENT

The authors gratefully acknowledge for support of the 2020 Research Grant and 2021 Research Publication given by the Engineering Faculty of Universitas Andalas. The first author is also grateful to the Structural Engineering Laboratory (SEL) of the Toyohashi University of Technology Japan and Prof. Shiro Kato that allowed the first author to use and develop several in-house computational programs owned by SEL for this study.

REFERENCES

[1] E. Satria, S. Kato, and Y. Niho. "Perbaikan metode perancangan struktur atap pada daerah rawan gempa," *Jurnal Teknik Mesin Indonesia*, BKSTM Indonesia (in Indonesian), vol. 10, no. 2, pp. 152-160, 2015.

[2] E. Satria *et al.,* "Study on dynamic behavior of a new type of two-way single layer lattice dome with nodal eccentricity," *Steel Compos. Struct.*, vol. 8, no. 6, pp. 511-530, 2008.

[3] T. Spuler, M. Brüninghold, and C.M. Galindo. "Pendulum-type bearings / seismic isolators – solutions and case studies," presented at 39th IABSE Symposium – Engineering the Future, Vancouver, Canada, 2017.

[4] M. Armali *et al.,* "Effectiveness of friction dampers in the seismic behavior of high-rise building vs shear wall system," *Eng. Rep.,* vol. 1, no. 2, pp. 1-14, 2019.

[5] N. Shedbale and P.V. Muley. "Review on viscoelastic materials used in viscoelastic dampers," *Int. Res. J. Eng. Technol. (IRJET)*, vol. 4, no. 7, pp. 3375-3381, 2017.

[6] Ras and M. Boumechra. "Seismic energy dissipation study of linear fluid viscous dampers in steel structure design." *AEJ-Alex. Eng. J.*, vol. 55, no. 3, pp. 2821-2832, 2016.

[7] K.S. Deore, R.S. Talikoti, and K.K. Tolani, "Vibration analysis of structure using tune mass damper," *Int. Res. J. Eng. Technol. (IRJET)*, vol. 4, no. 7, pp. 2814-2820, 2017.

[8] F. Rahimi, R. Aghayari, and B. Samali, "Application of tuned mass dampers for structural vibration control: A state-of-the-art review," *Civ. Eng. J.,* vol. 6, no. 8, pp. 1622-1651, 2020.

[9] A.M. Aly, "Vibration control of high-rise buildings for wind: a robust passive and active tuned mass damper," *Smart Struct. Syst.*, vol. 13, no. 3, pp. 473-500, 2014.

[10] Z. Zhou, "Effectiveness of tuned mass dampers in mitigating earthquake ground motions in low and medium rise buildings," M. S. thesis, Rutgers University, New Jersey, 2014.

[11] G.W. Housner *et al.,* "Structural control: past, present, and future," *J. Eng. Mech.*, vol. 123, no. 9, pp. 897-971, 1997.

[12] J. Jia, *Dynamic absorber - Modern Earthquake Engineering*, Berlin: Springer, 2017, pp. 743-782, doi:10.1007/978-3-642-31854-2_24.

[13] S. Elias, V. Matsagar, and T.K. Datta, "Distributed tuned mass dampers for multi-mode control of benchmark building under seismic excitations," *J. Earthq. Eng.,* vol. 23, no. 7, pp. 1137-1172, 2019.

[14] L. Suresh and K.M. Mini, "Effect of multiple tuned mass dampers for vibration control in high-rise buildings," *Pract. Period. Struct. Des. Constr.*, vol. 24, no. 4, pp. 04019031, 2019.

[15] J. Velicko and L. Gaile, "Overview of tuned liquid dampers and possible ways of oscillation damping properties improvement," In Proceedings of the 10th International Scientific and Practical Conference, 2015, pp. 233-238.

[16] A. Farshidianfar, P. Oliazadeh, and H.R. Farivar, "Optimal parameter's design in tuned liquid column damper," presented at 17th Annual Conference on Mechanical Engineering-ISME2009, University of Tehran, Iran, 2009.

[17] L. Son, M. Bur, and E. Satria, "Vibration response suppression of space structure using two u-shaped water container," *Int. J. Adv. Sci. Eng. Inf. Technol.*, vol. 8, no. 6, pp. 2472-2478, 2018.

[18] B.J. Park *et al.*, "Vibration control of a structure by a tuned liquid column damper with embossments," *Eng. Struct.,* vol. 168, pp. 290-299, 2018.

[19] L. Son *et al.*, "Design of double dynamic vibration absorbers for reduction of two DOF vibration system," *Struct. Eng. Mech.,* vol. 57, no. 1, pp. 161-178, 2016.

[20] A. Di Matteo, A. Pirotta, and S. Tumminelli, "Combining TMD and TLCD: Analytical and experimental studies," *J. Wind Eng. Ind. Aerodyn.*, vol. 167, pp. 101-113, 2017.

[21] R. Aghlara, M.M. Tahir, and A. Adnan. "Comparative study of eight metallic yielding damper," *Jurnal Teknologi Universiti Teknologi Malaysia*, vol. 77, no. 16, pp. 119-125, 2015.

[22] Z. Javanmardi *et al.*, "State-of-the-art review of metallic dampers: testing, development, and implementation," *Archives of Computational Methods in Engineering*, vol. 27, pp. 455-478, 2020.

[23] E. Satria *et al.*, "Static and dynamic analysis of steel U-damper for space structures," *Int. J. Adv. Sci. Eng. Inf. Technol.*, vol. 8, no. 1, pp. 212-218, 2018.

[24] S. Kato *et al.*, "Simulation of the cyclic behavior of j-shaped steel hysteresis devices and study on the efficiency for reducing earthquake responses of space structures," *J. Constr. Steel Res.*, vol. 61, no. 10, pp. 1457-1473, 2006.

[25] S. Kato and Y.B. Kim, "A finite element parametric study on the mechanical properties of J-shaped steel hysteresis devices," *J. Constr. Steel Res.*, vol. 62, no. 8, pp. 802-811, 2006.